

Linkage Isomerization Reactions of $M(\text{CO})_2\text{L}$ Complexes ($M = (\eta^5\text{-C}_5\text{H}_5)\text{Mn}$, $(\eta^5\text{-C}_5\text{H}_5)\text{Re}$, or $(\eta^6\text{-C}_6\text{H}_6)\text{Cr}$; $L = 2,3\text{-Dihydrofuran}$): A Step-Scan FTIR and DFT Study

Ashfaq A. Bengali,^{*,†} Michael B. Hall,^{*,‡} and Hong Wu[‡]

Department of Chemistry, Texas A&M University at Qatar, P.O. Box 23874, Doha, Qatar, and Department of Chemistry, Texas A&M University, College Station, Texas 77843-3255

Received May 20, 2008

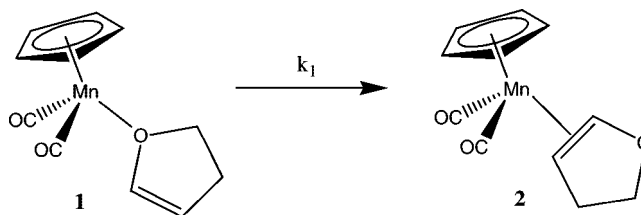
The linkage isomers, $M(\text{CO})_2\text{-}(\eta^1\text{-O})\text{-}2,3\text{ DHF}$ and $M(\text{CO})_2\text{-}(\eta^2\text{-C,C})\text{-}2,3\text{ DHF}$ [$M = (\eta^5\text{-C}_5\text{H}_5)\text{Mn}$, $(\eta^5\text{-C}_5\text{H}_5)\text{Re}$, $(\eta^6\text{-C}_6\text{H}_6)\text{Cr}$; DHF = dihydrofuran] are formed upon photolysis of the parent $M(\text{CO})_3$ complexes in the presence of 2,3-DHF. The rearrangement of the oxygen bound to the thermodynamically favored π bound complex is followed on the millisecond to microsecond time scale using step-scan FTIR. The rate of the isomerization reaction increases in the order $\text{Re} < \text{Mn} < \text{Cr}$ primarily due to a decrease in the activation enthalpy. The experimental data along with theoretical calculations suggest that the rearrangement proceeds intramolecularly in which the metal migrates from one functional group to another.

Introduction

Photolysis of metal carbonyl complexes with ultraviolet light results in the loss of a CO ligand and formation of highly reactive 16 electron intermediates.¹ Gas phase studies have shown that these transients react with a variety of ligands at gas kinetic rates with relatively little selectivity.² In the condensed phase, the coordinatively unsaturated species are solvated within picoseconds of CO loss.³ Because of the high reactivity and low selectivity of the unsaturated metal complexes, the possibility exists for the formation of linkage isomers upon photolysis of metal carbonyls in solvents with more than one potential binding site.

Previous studies have reported the formation of linkage isomers upon photolysis of organometallic complexes in solution phase, and some have reported the dynamics of the isomerization process.⁴ Most of these studies have focused on the $M(\text{CO})_5$ ($M = \text{Cr}$, Mo , or W) system. For example, Schultz and co-workers studied the formation and subsequent isomerization of $(\text{CO})_5\text{M-}(\eta^1\text{-O})\text{-}2,5\text{ DHF}$ to the carbon bound $(\text{CO})_5\text{M-}(\eta^2\text{-C,C})\text{-}2,5\text{ DHF}$ complex [$M = \text{Cr}$, Mo , or W ; DHF = dihydrofuran].^{4e,g} Both the kinetics and the thermodynamics of

Scheme 1



the reaction were studied. The isomerization followed an intramolecular pathway, and the η^2 bound isomer was found to be the thermodynamic product, although the reaction was almost thermoneutral. While investigating the displacement of η^2 bound furan and 2,3-DHF from the $\text{CpMn}(\text{CO})_2$ fragment ($\text{Cp} = \eta^5\text{-C}_5\text{H}_5$), we were surprised to observe the formation and conversion of the oxygen bound DHF adduct, $\text{CpMn}(\text{CO})_2\text{-}(\eta^1\text{-O})\text{-}2,3\text{ DHF}$ (**1**), to the $\text{CpMn}(\text{CO})_2\text{-}(\eta^2\text{-C,C})\text{-}2,3\text{ DHF}$ (**2**) complex (Scheme 1).

This observation provided us with an opportunity to study the dynamics of a linkage isomerization reaction for the group 7 metals, a rearrangement which has not received much attention.⁴ⁱ We present in this article an experimental and theoretical investigation into the formation and subsequent isomerization of $[\text{M}]\text{-}(\eta^1\text{-O})\text{-}2,3\text{ DHF}$ to the $[\text{M}]\text{-}(\eta^2\text{-C,C})\text{-}2,3\text{ DHF}$ complex ($[\text{M}] = \text{CpMn}(\text{CO})_2$, $(\eta^6\text{-C}_6\text{H}_6)\text{Cr}(\text{CO})_2$, or $\text{CpRe}(\text{CO})_2$).

Experimental and Theoretical Details

All experiments were conducted using a Bruker Vertex 80 FTIR with both rapid and step-scan capabilities. The samples were photolyzed with either 355 or 266 nm light from a Nd:YAG laser operating at 1 Hz. For the step scan experiments, the solution was flowed through a temperature controlled CaF_2 cell (0.5 mm) to ensure that a fresh sample was photolyzed by each laser shot. The temperature was monitored by inserting a thermocouple tip into the circulating solution at the exit of the IR cell. All reagents were of >97% purity. The cyclohexane (EMD) was anhydrous grade, and 2,3-DHF (Alfa-Aesar) was freshly distilled from CaH_2 . The metal complexes (Strem and Alfa-Aesar) were used as received.

* To whom correspondence should be addressed. E-mail: ashfaq.bengali@qatar.tamu.edu.

[†] Texas A&M University at Qatar.

[‡] Texas A&M University.

(1) Hall, C.; Perutz, R. N. *Chem. Rev.* **1996**, 3125.

(2) (a) Wang, W.; Jin, P.; Liu, Y.; She, Y.; Fu, K.-J. *J. Phys. Chem.* **1992**, 96, 9821. (b) Weitz, E. *J. Phys. Chem.* **1987**, 91, 3945. (c) Fletcher, T. R.; Rosenfeld, R. N. *J. Am. Chem. Soc.* **1983**, 105, 6358. (d) Fletcher, T. R.; Rosenfeld, R. N. *J. Am. Chem. Soc.* **1986**, 108, 1686.

(3) Simon, J. D.; Xie, X. *J. Phys. Chem.* **1986**, 90, 6751.

(4) (a) Xie, X.; Simon, J. D. *J. Phys. Chem.* **1989**, 93, 4401. (b) Spradling, M. D.; Dobson, G. R. *Inorg. Chem.* **1990**, 29, 880. (c) Zhang, S.; Dobson, G. R.; Brown, T. L. *J. Am. Chem. Soc.* **1991**, 113, 6908. (d) Ladogana, S.; Suresh, K. N.; Smit, J. P.; Dobson, G. R. *Inorg. Chem.* **1997**, 36, 650. (e) Elgamiel, R.; Huppert, I.; Lancry, E.; Yerucham, Y.; Schultz, R. H. *Organometallics* **2000**, 19, 2237. (f) To, T. T.; Barnes, C. E.; Burkey, T. J. *Organometallics* **2004**, 23, 2708. (g) Shagal, A.; Schultz, R. H. *Organometallics* **2007**, 26, 4896. (h) Bitterwolf, T. E. *Coord. Chem. Rev.* **2006**, 250, 1196. (i) To, T. T.; Duke, C. B.; Junker, C. S.; O'Brien, C. M.; Ross, C. R.; Barnes, C. E.; Webster, C. W.; Burkey, T. J. *Organometallics* **2008**, 27, 289.

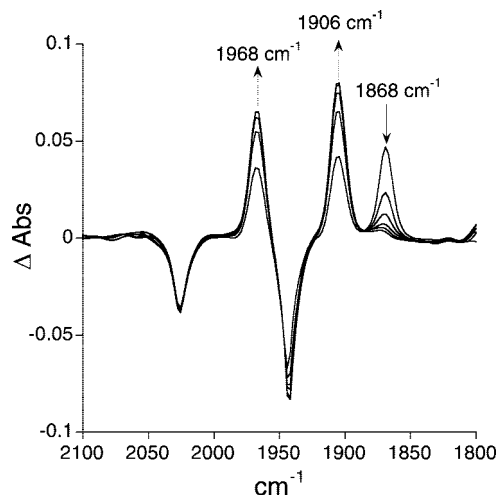


Figure 1. Difference step-scan FTIR spectrum obtained upon photolysis of a cyclohexane solution of $\text{CpMn}(\text{CO})_3$ with [2,3-DHF] = 1 M at 302 K. Spectra shown were obtained at 2.5 ms intervals.

Table 1. Experimental and Calculated CO Stretching Frequencies for the Observed Complexes

	[M]	$\nu_{\text{CO}}([\text{M}]-(\eta^1\text{-O-2,3-DHF}) \text{ cm}^{-1})$	$\nu_{\text{CO}}([\text{M}]-(\eta^2\text{-C, C-2,3-DHF}) \text{ cm}^{-1})$
CpMn(CO) ₂	experimental	1868	1906, 1968
	calculated	1989, 2043	2007, 2051
	scaled (0.95 × calculated)	1890, 1941	1907, 1948
BzCr(CO) ₂	experimental	1844, 1895	1869, 1921
	calculated	1961, 2000	1972, 2009
	scaled (0.95 × calculated)	1863, 1900	1873, 1909
CpRe(CO) ₂	experimental	1858, 1925	1902, 1973
	calculated	1950, 2007	1982, 2039
	scaled (0.95 × calculated)	1853, 1907	1883, 1937

The reactions were monitored over a 20 to 30 °C temperature range. The errors reported in the activation parameters were obtained from linear least-squares fits to the available data.

The energetics of the isomerization reactions were studied using the Gaussian 03 program⁵ employing the B3LYP functional.⁶ The transition metal atoms were described by the LANL2DZ basis set⁷ with the effective core potential replaced by Couty and Hall's optimized split valence function.⁸ The cc-pVDZ basis set was used for the H, C, and O atoms.⁹

Results and Discussion

(a). CpMn(CO)₃. As shown in Figure 1, photolysis of a 3–4 mM cyclohexane solution of $\text{CpMn}(\text{CO})_3$ in the presence of 1 M 2,3-DHF results in the formation of both complexes **1** and **2**. The identity of these complexes is verified by the location of the respective CO stretching absorbances. For example, as shown in Table 1, **1** has a CO stretching absorption at 1868 cm^{-1} (the second CO band is obscured by the parent Cp-

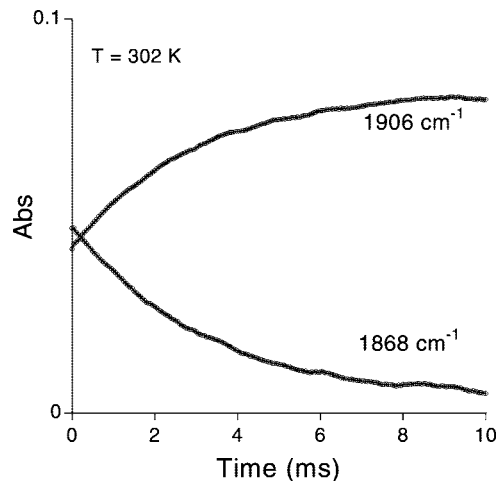


Figure 2. Absorbance vs time profiles for complexes **1** and **2** obtained upon photolysis of $\text{CpMn}(\text{CO})_3$ in a cyclohexane solution in the presence of 1 M 2,3-DHF at 302 K.

Table 2. Isomerization Rate Constants at 295 K and Associated Activation Parameters

metal	k_1 (s^{-1})	ΔH^\ddagger (kcal/mol) ^a	ΔH^\ddagger (kcal/mol) ^b	ΔS^\ddagger (e.u.) ^a
Mn	163 ± 10	15.4 ± 0.6	12.5	$+4.0 \pm 2.0$
Cr	12300 ± 200	12.2 ± 0.4	9.7	$+2.0 \pm 0.4$
Re	24.0 ± 2.0	17.0 ± 0.7	14.6	$+6.0 \pm 2.0$

^a Experimental data. ^b Calculated data.

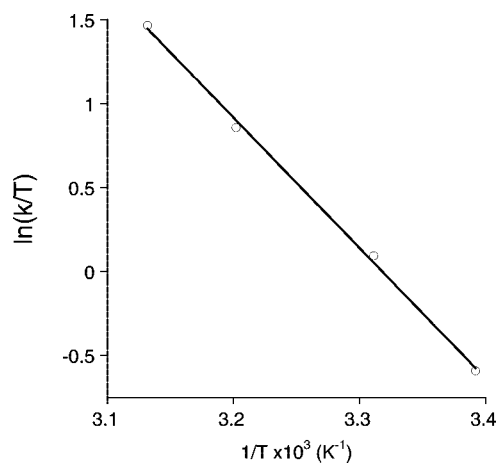


Figure 3. Eyring plot for the conversion of complex **1** to **2**.

$\text{Mn}(\text{CO})_3$ absorbance at 1943 cm^{-1}) similar to that observed for the well established $\text{CpMn}(\text{CO})_2(\text{THF})$ complex at 1864 and 1936 cm^{-1} .¹⁰ The bands at 1906 and 1968 cm^{-1} are assigned to complex **2** by analogy with the $\text{CpMn}(\text{CO})_2(\eta^2\text{-cyclopentene})$ complex, which exhibits CO stretching absorbances at 1905 and 1965 cm^{-1} .^{10a} Furthermore, as mentioned previously, similar oxygen bound and η^2 carbon bound complexes have been observed in the case of the $\text{M}(\text{CO})_5$ (M = Cr, Mo, or W) fragments.^{4e,g}

Assuming that the absorption coefficients for **1** and **2** are similar, the nearly identical intensities of the CO stretching bands immediately after photolysis suggest that the initially formed $\text{CpMn}(\text{CO})_2(\text{CyH})$ [CyH = cyclohexane] complex is not very

(5) Frisch, M. J. et al. *Gaussian 03*, revisions B and B.05; Gaussian Inc.: Wallingford, CT, 2004.

(6) (a) Becke, A. D. *J. Phys. Chem.* **1993**, *98*, 5648. (b) Lee, C.; Yang, W.; Parr, R. G. *Phys. Rev. B* **1988**, *37*, 785.

(7) Hay, P. J.; Wadt, W. R. *J. Chem. Phys.* **1985**, *82*, 270.

(8) Couty, M.; Hall, M. B. *J. Comput. Chem.* **1996**, *17*, 1359.

(9) (a) Dunning, T. H. *J. Phys. Chem.* **1989**, *90*, 1007. (b) Woon, D. E.; Dunning, T. H., Jr. *J. Chem. Phys.* **1994**, *100*, 2975.

(10) (a) Lugovskoy, S.; Lin, J.; Schultz, R. H. *J. Chem. Soc., Dalton Trans.* **2003**, 3103. (b) Yang, P.-F.; Yang, G. K. *J. Am. Chem. Soc.* **1992**, *114*, 6937. (c) Coleman, J. E.; Dulaney, K. E.; Bengali, A. A. *J. Organomet. Chem.* **1999**, *572*, 65.

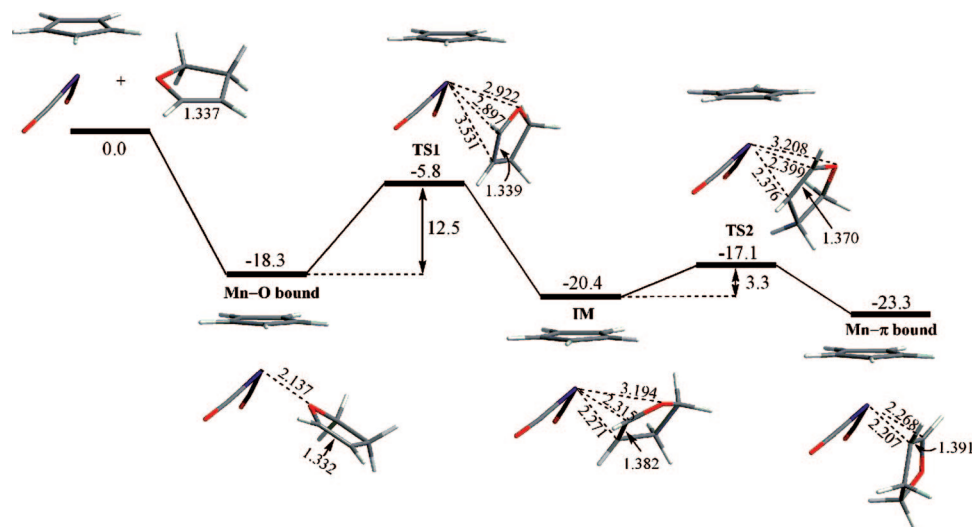


Figure 4. Enthalpy diagram showing the mechanism of the isomerization reaction, **1** \rightarrow **2**, determined from DFT calculations.

Table 3. Calculated Enthalpies for the Isomerization Reactions^a

reaction	ΔH (kcal/mol)		
	CpMn(CO) ₂	BzCr(CO) ₂	CpRe(CO) ₂
[M] + 2,3 DHF \rightarrow M-O bound	-18.3	-14.0	-22.4
[M] + 2,3 DHF \rightarrow IM	-20.4	-15.3	-37.1
[M] + 2,3 DHF \rightarrow M- π bound	-23.3	-16.4	-39.1
[M]-O bound \rightarrow TS1	12.5 (15.4)	9.7 (12.2)	14.6 (17.0)
IM \rightarrow TS1	14.6	11.0	29.3
IM \rightarrow TS2	3.3	2.6	3.7
[M]- π bound \rightarrow TS2	6.2	3.7	5.7

^a Numbers in parenthesis are the experimental values.

selective in its reaction with either the oxygen atom or the π bond of the 2,3 DHF ligand.¹¹ This conclusion is consistent with previous studies which reported less than a factor of 2 difference in the rate constant for the reaction of CpMn(CO)₂(CyH) with THF and cyclopentene.^{10a}

Upon formation, the kinetic product **1** converts to the thermodynamically favored isomer **2**. As shown in Figure 2, complex **1** undergoes a first order decay with a half-life of 2 ms at 302 K, and **2** grows in at the same rate. Interestingly, the rate of this isomerization is almost independent of the concentration of 2,3-DHF. Thus, when CpMn(CO)₃ is photolyzed in neat 2,3-DHF (13 M), the rate of conversion is only a factor of 2 slower than when [2,3-DHF] = 1 M. The minimal effect of [2,3-DHF] on the reaction rate suggests that the isomerization proceeds through an intramolecular pathway. However, this observation alone is not sufficient to rule out a possible reversible dissociation of the oxygen bound ligand from the Mn center followed by nonreversible binding of DHF to form **2** since in this case, the resulting CpMn(CO)₂ fragment would be reacting with 2,3-DHF to form either **1** or **2**. Consequently, the rate constant for the isomerization would be independent of [2,3-DHF]. However, activation parameters (shown in Table 2) obtained from an Eyring analysis shown in Figure 3, together with DFT calculations discussed below, indicate an intramolecular pathway for the isomerization reaction.

The results show that an enthalpic barrier of 15.4 ± 0.6 kcal/mol separates **1** from **2**. This activation enthalpy is considerably lower than the 24–25 kcal/mol estimate for the strength of the CpMn(CO)₂-THF bond.^{10b,c} While the oxygen atom in 2,3-DHF

is expected to be a weaker donor than that in THF, the large difference between the activation enthalpy and the Mn-THF bond strength indicates that the isomerization does not involve complete dissociation of the Mn–O bond. The slightly positive activation entropy is also consistent with this conclusion. It is therefore likely that the isomerization reaction proceeds intramolecularly in which the metal migrates from one functional group to another. A similar mechanism has also recently been proposed for other linkage isomerization reactions.⁴ⁱ

(b). (η^6 -C₆H₆)Cr(CO)₃ and CpRe(CO)₃. Photolysis of both BzCr(CO)₃ [Bz = (η^6 -C₆H₆)] and CpRe(CO)₃ under identical conditions also results in the formation of the respective oxygen bound and η^2 carbon bound isomers with subsequent conversion of the η^1 complex to the more thermodynamically favored η^2 isomer. Interestingly, the conversion of BzCr(CO)₂(η^1 -(O)-2,3 DHF) (**3**) to BzCr(CO)₂(η^2 -(C,C)-2,3 DHF) (**4**) is almost 70 times faster, while that of CpRe(CO)₂(η^1 -(O)-2,3 DHF) (**5**) to CpRe(CO)₂(η^2 -(C,C)-2,3 DHF) (**6**) is seven times slower than the isomerization of complex **1** to **2**. Data shown in Table 2 indicates that the differences in reactivity are primarily due to enthalpic effects. The experimental activation enthalpies of 12.2 kcal/mol (**3** to **4**) and 17.0 kcal/mol (**5** to **6**) are consistent with the binding strengths of weak ligands to the Cr and Re centers relative to Mn. For example, the BzCr(CO)₂-THF bond is estimated to be 3 kcal/mol weaker than the CpMn(CO)₂-THF interaction.^{10b,c,12} Similarly, as is often the case with third row metals relative to their first row congeners, the CpRe(CO)₂(η^2 -benzene) bond is almost 5 kcal/mol stronger than the analogous CpMn(CO)₂(η^2 -toluene) interaction.^{13,14} The observation that the trend in the activation enthalpies for the isomerization reaction mirror those of the metal–ligand binding energies suggests that there is relatively more metal–(η^1 -(O)-2,3 DHF) bond breaking than metal–(η^2 -(C,C)-2,3 DHF) bond making in the transition state.

Unlike the group 6 pentacarbonyl complexes,^{4e,g} a measurable equilibrium is not established between the two isomers indicating that the π bound complex is relatively more stable (by at least a few kcal/mol) than the oxygen bound adduct. This observation is perhaps not surprising since the group 6 pentacarbonyls are expected to be more electron deficient than the Cr, Mn, and Re complexes resulting in a relatively more stable

(11) The conversion of the CpMn(CO)₂(CyH) complex to **1** and **2** occurs on a timescale that is faster than that of the isomerization reaction. Thus, this reaction is not directly observed in the present study.

(12) Bengali, A. A.; Fehnel, R. *Organometallics* **2005**, *24*, 1156.

(13) Bengali, A. A. *Organometallics* **2000**, *19*, 4000.

(14) Bengali, A. A.; Leicht, A. *Organometallics* **2001**, *20*, 1345.

interaction with the σ donor oxygen atom of the DHF ligand and a weaker η^2 interaction with the π bond due to reduced contribution from π backbonding. Calculations employing density functional theory were performed to better understand the energetics and the nature of the structures involved in the rearrangement process.

(c). DFT Calculations. After full optimization of the geometries of the stable isomers and the transition states connecting them, frequency calculations were performed to verify the nature of the critical points reached in the optimization. The calculated frequencies (both unscaled and scaled) in the CO region are reported in Table 1. These are in reasonable agreement with the experimental values with the expected mean error of about $10\text{--}30\text{ cm}^{-1}$ for the scaled frequencies.¹⁵ Consistent with the experimental results, the stretching frequencies of the η^2 bound isomer are higher than those of the η^1 -O bound isomer, a result that reflects the ligand's acceptor properties in the former isomer and the net stronger donor properties in the latter isomer. Consistent with the experimental findings, the calculations suggest that the metal migrates from one functional group to another forming a transition state with considerable lengthening of the M–O bond (Figure 4). The calculated activation enthalpies shown in Table 3 are in good agreement with the experimental values. Interestingly, there appears to be an unstable intermediate (IM) along the reaction coordinate, which undergoes rotation about the coordinated π bond to form the final thermodynamically favored metal– π bound isomer.

Consistent with previous experimental estimates for weak metal–solvent bond enthalpies,^{10c,12–14} the binding strength of the DHF ligand (both η^1 and η^2 bound isomers) increases in the order $\text{Cr} < \text{Mn} < \text{Re}$ (Table 3). There is also a notable difference in the relative stabilities of the Mn– π bound and

Re– π bound complexes (16 kcal/mol). The calculated C=C bond length in the Re– π complex is longer than that in the analogous Mn complex (1.418 Å vs 1.391 Å), indicating that the origin of this large difference in stability is likely due to increased π donation and backbonding in the Re complex. A greater degree of synergistic bonding in the Re complex is also evident in the relative stabilities of the Re– η^1 -O and Re– η^2 -(C,C) isomers. In the case of the Mn and Cr centers, the π bound isomer is calculated to be only 2–5 kcal/mol more stable than the oxygen bound complex, while for Re, this difference is almost 17 kcal.

Conclusions

Photolysis of $\text{CpMn}(\text{CO})_3$, $\text{CpRe}(\text{CO})_3$, and $(\eta^6\text{-C}_6\text{H}_6)\text{Cr}(\text{CO})_3$ in the presence of 2,3 dihydrofuran results in the loss of a CO ligand and the formation of the corresponding metal–(η^1 -O)-2,3 DHF and metal–(η^2 -(C,C))-2,3 DHF linkage isomers. The conversion of the oxygen bound complex to the thermodynamically favored π bound adduct is observed. The rate of the isomerization reaction increases in the order $\text{Re} < \text{Mn} < \text{Cr}$ primarily due to a decrease in the activation enthalpy. The rearrangement proceeds by an intramolecular process in which the metal migrates from one functional group to another. Theoretical calculations predict activation enthalpies consistent with the experimental results and the presence of an unstable π bound intermediate along the reaction coordinate, which undergoes rotation about the coordinated π bond to form the final thermodynamically favored metal– π bound isomer.

Supporting Information Available: Calculated enthalpy diagrams for the isomerization of $3 \rightarrow 4$ and $5 \rightarrow 6$, and measured experimental values of k_{obs} for the isomerizations at all temperatures studied. This material is available free of charge via the Internet at <http://pubs.acs.org>.

OM800457D

(15) Cramer, C. J. *Essentials of Computational Chemistry*; John Wiley & Sons Ltd: New York, 2002; p. 305.